Cell Death and Differentiation (2016) 23, 313–322

www.nature.com/cdd

The SR/ER-mitochondria calcium crosstalk is regulated by GSK3β during reperfusion injury

L Gomez*[,1,2,4], P-A Thiebaut[1,4], M Paillard[1], S Ducreux[1], M Abrial[1], C Crola Da Silva[1], A Durand[1], MR Alam[1], F Van Coppenolle[1], S-S Sheu[2] and M Ovize[1,3]

Glycogen synthase kinase-3β (GSK3β) is a multifunctional kinase whose inhibition is known to limit myocardial ischemia–reperfusion injury. However, the mechanism mediating this beneficial effect still remains unclear. Mitochondria and sarco/endoplasmic reticulum (SR/ER) are key players in cell death signaling. Their involvement in myocardial ischemia–reperfusion injury has gained recognition recently, but the underlying mechanisms are not yet well understood. We questioned here whether GSK3β might have a role in the Ca^{2+} transfer from SR/ER to mitochondria at reperfusion. We showed that a fraction of GSK3β protein is localized to the SR/ER and mitochondria-associated ER membranes (MAMs) in the heart, and that GSK3β specifically interacted with the inositol 1,4,5-trisphosphate receptors (IP_3Rs) Ca^{2+} channeling complex in MAMs. We demonstrated that both pharmacological and genetic inhibition of GSK3β decreased protein interaction of IP_3R with the Ca^{2+} channeling complex, impaired SR/ER Ca^{2+} release and reduced the histamine-stimulated Ca^{2+} exchange between SR/ER and mitochondria in cardiomyocytes. During hypoxia reoxygenation, cell death is associated with an increase of GSK3β activity and IP_3R phosphorylation, which leads to enhanced transfer of Ca^{2+} from SR/ER to mitochondria. Inhibition of GSK3β at reperfusion reduced both IP_3R phosphorylation and SR/ER Ca^{2+} release, which consequently diminished both cytosolic and mitochondrial Ca^{2+} concentrations, as well as sensitivity to apoptosis. We conclude that inhibition of GSK3β at reperfusion diminishes Ca^{2+} leak from IP_3R at MAMs in the heart, which limits both cytosolic and mitochondrial Ca^{2+} overload and subsequent cell death.
Cell Death and Differentiation (2016) **23,** 313–322; doi:10.1038/cdd.2015.101; published online 24 July 2015

Glycogen synthase kinase-3 (GSK3) was originally identified as a phosphorylating kinase for glycogen synthase.[1,2] It has two isoforms, α and β, that possess strong homology in their kinase domains with, however, distinct functions.[3] GSK3 is constitutively active but it can be inhibited by phosphorylation on serine 21 (Ser21) for GSK3α and Ser9 for GSK3β.[4] In the heart, GSK3β has several important roles in cardiac hypertrophy[5] and ischemia–reperfusion (IR) injury.[6] Accumulating evidence indicates that phospho-Ser9-GSK3β-mediated cytoprotection is achieved by an increased threshold for permeability transition pore (PTP) opening.[6–9] The mechanism by which GSK3β delays PTP opening still remains unclear. It has been reported that GSK3β could interact with ANT at the inner mitochondrial membrane in the heart[9] and/or to phosphorylate voltage-dependent anion channel (VDAC) and cyclophilin D (CypD) in cancer cells.[10,11] GSK3β also has other proposed mechanisms of action, including a poorly characterized role in calcium (Ca^{2+}) homeostasis regulation[12] and protein–protein interactions,[9] as well as functions in different subcellular fractions such as the nucleus, cytosol and mitochondria.[13]

Reperfusion is the most powerful intervention to salvage ischemic myocardium. However, it can also paradoxically lead to cardiomyocyte injury and death.[14] One of the main actors of this lethal reperfusion injury is cellular Ca^{2+} overload,[15] which results in part from excessive sarco/endoplasmic reticulum (SR/ER) Ca^{2+} release and Ca^{2+} influx through the plasma membrane (e.g. through L-type Ca^{2+}channel and NCX (sodium-calcium exchanger)).[16] Although ryanodine receptors (RyRs) are the major cardiac SR/ER Ca^{2+}-release channels involved in excitation–contraction coupling (ECC)[17] and ischemia–reperfusion (IR) injury,[18] recent studies reported an increasing role for inositol 1,4,5-trisphosphate receptors (IP_3Rs) Ca^{2+}-release channels in the modulation of ECC and cell death.[19,20] Ca^{2+}-handling proteins of ER and mitochondria are highly concentrated at mitochondria-associated ER membranes (MAMs), providing a direct and proper mitochondrial Ca^{2+} signaling, including VDAC, Grp75 and IP_3R1.[20–22]

Here, we provide evidence that, following IR, a fraction of cellular GSK3β is localized at the SR/ER and MAMs. At the MAMs interface, GSK3β can specifically interact and regulate the protein composition of the IP_3R Ca^{2+} channeling complex

[1]INSERM UMR-1060, Laboratoire CarMeN, Université Lyon 1, Faculté de medicine, Rockefeller et Charles Merieux Lyon-Sud, Lyon 69003, France; [2]Department of Medicine, Center for Translational Medicine, Sidney Kimmel College, Thomas Jefferson University, Philadelphia, PA 19107, USA and [3]Hospices Civils de Lyon, Hôpital Louis Pradel, Service d'Explorations Fonctionnelles, Cardiovasculaires and CIC de Lyon, Lyon 69394, France
*Corresponding author: L Gomez, INSERM UMR-1060, Laboratoire CarMeN, Université Lyon 1, Faculté de Medicine, Rockefeller et Charles Merieux Lyon-Sud, Lyon 69003, France. Tel: +33 4 78 77 70 47; Fax: +33 4 78 77 71 75; E-mail: ludovic.gomez@inserm.fr
[4]These authors contributed equally to this work.

Abbreviations: ANT, adenine nucleotide translocator; Ca^{2+}, calcium; CTRL, control; CypD, cyclophilin D; ER, endoplasmic reticulum; GSK3β, glycogen synthase kinase-3β; HR, hypoxia reoxygenation; MAM, mitochondria-associated ER membranes; MTS, mitochondrial targeting sequence; PTP, permeability transition pore; IP_3R, inositol 1,4,5-trisphosphate receptor; IR, ischemia–reperfusion; RyR, ryanodine receptor; SB21, SB216763; Ser, serine; SR/ER, sarco/endoplasmic reticulum; Tyr, tyrosine; VDAC, voltage-dependent anion channel; WT, wild type

Received 09.6.15; accepted 22.6.15; Edited by L Scorrano; published online 24.7.15

and modulate Ca^{2+} transfer between SR/ER and mitochondria. These findings support a novel mechanism of action of GSK3β in cell death process during reperfusion injury.

Results

GSK3β interacts with the IP_3R Ca^{2+} channeling complex at the SR/ER-mitochondria interface in the heart. To characterize the role of GSK3β in the heart, we first determined its subcellular localization. The purity of SR/ER, mitochondrial and MAM fractions from mouse hearts were visualized by both electron microscopy (Supplementary Figure S1) and validated by western blot (WB) (Figure 1a). GSK3β was detected in both SR/ER and mitochondria and more particularly in the MAMs fraction together with IP_3R, Grp75, VDAC and CypD. To characterize the implication of GSK3β in MAM fraction, we performed two-dimensional blue native page separation on heart homogenates. Our results showed that although GSK3β was present in varying amounts in complexes, a pool of GSK3β was also present in a higher molecular weight complex encompassing IP_3R, Grp75, VDAC and CypD (Figure 1b, arrow), suggesting that GSK3β interacts with MAM-resident proteins to form a macrocomplex in native state in the heart.

To confirm the involvement of GSK3β in MAM protein complex, we next investigated its relationship with CypD, VDAC, Grp75 and IP_3R at the MAM interface.[21] Using *in situ* proximity ligation assay (PLA), we first validated that GSK3β interacted with IP_3R, Grp75, VDAC or CypD but not RyR2 and ANT in both adult cardiomyocytes and H9c2 cells (Supplementary Figure S2A). GSK3β inhibitors were used to determine if it might change these protein interactions. As shown in Supplementary Figures S2A and B, both pharmacological and genetic inhibition of GSK3β decreased the interaction of GSK3β with IP_3R, Grp75, VDAC or CypD. Interestingly, the inhibition of GSK3β also modified the interaction between the other partner proteins of the complex; indeed, SB216763 (SB21) significantly reduced the co-immunoprecipitation (IP) of IP_3R with GSK3β, as well as Grp75, VDAC and CypD in heart homogenates (Figure 1c). In line with this, using PLA approach, adult cardiomyocytes treated with SB21 displayed significantly decreased interaction of GSK3β, Grp75, VDAC and CypD with IP_3R (Figure 1d). Altogether, these results suggest that GSK3β modulates the IP_3R-Ca^{2+} channeling complex at the MAM interface in the heart.

Inhibition of GSK3β alters Ca^{2+} transfer from SR/ER to mitochondria in cardiomyocytes. We next examined the role of GSK3β on the transfer of Ca^{2+} between SR/ER and mitochondria. Calcium fluxes were monitored in isolated adult mouse cardiomyocytes stained with rhod-2 fluorescent dye. In our model, fluorescent dye showed a specific mitochondrial staining, overlapping with the mitochondrial marker Mitotracker Green (Figure 2a). The quantitative pixel-by-pixel analysis measured with Zen software (Zeiss, Germany) showed strong correlation between rhod-2 and Mitotracker Green with an overlap coefficient averaging 0.89 ± 0.01 (0 corresponds to no overlap and 1 corresponds to a perfect overlap) (Figure 2a). Under basal conditions, 100 μM histamine induced a transient Ca^{2+} release from SR/ER, which consequently induced mitochondrial Ca^{2+} uptake in adult cardiomyocytes (Figure 2b), reflecting the IP_3R-mediated Ca^{2+} transfer from SR/ER to mitochondria. This Ca^{2+} transfer was significantly reduced when GSK3β was inhibited by SB21 averaging 0.60 ± 0.06- *versus* 1.00 ± 0.07-fold *versus* control (CTRL); $P < 0.05$ (Figure 2b). Interestingly, the inhibition of GSK3β by SB21 did not modify the caffeine-induced Ca^{2+} transfer from SR/ER to mitochondria ($P =$ NS, Figure 2c), suggesting that GSK3β has a specific action on IP_3R channels with no effect on RyRs in adult cardiomyocytes. As adult mice cardiomyocytes are refractory to transfection using conventional methods and that they can only be maintained in culture for short periods before they dedifferentiate,[23] the analysis on adult cardiomyocytes was complemented by a number of assays on H9c2 cells to define the role of GSK3β in the regulation of Ca^{2+} transfer between SR/ER and mitochondria. Similar to adult cardiomyocytes, rhod-2 showed a specific mitochondrial staining in H9c2 cells with an overlap coefficient averaging 0.87 ± 0.02 when compared with Mitotracker Green (Supplementary Figure S3A). As shown previously, SB21 did not modulate the mitochondrial Ca^{2+} amplitude induced by caffeine ($P =$ NS, Supplementary Figure S3B), but significantly reduced the Ca^{2+} transfer under histamine stimulation in H9c2 cells (Supplementary Figures S3C and S5). Although the knockdown of GSK3β significantly reduced the amplitude of Ca^{2+} into mitochondria averaging 0.36 ± 0.01- *versus* 1.00 ± 0.10-fold with SiC; $P < 0.05$ (Supplementary Figure S3D), the overexpression of GSK3β in H9c2 cells significantly enhanced the Ca^{2+} transfer into mitochondria when compared with its respective control averaging 1.52 ± 0.07 *versus* 1.00 ± 0.04 in the pcDNA group; $P < 0.05$ (Supplementary Figure S3E). These results were further confirmed using a mitochondrially targeted Ca^{2+} probe (Mitycam, Glasgow, Scotland, UK), suggesting that GSK3β specifically controls and regulates the IP_3R-mediated SR/ER Ca^{2+} transfer to mitochondria in cardiac cells.

To rule out a potential depolarization of mitochondria under GSK3β inhibition, we stained cardiac cells with TMRM to analyze mitochondrial membrane potential. Neither the pharmacological nor the genetic inhibition of GSK3β modified the mitochondrial membrane potential of cells (Supplementary Figures S4A and B), indicating that the observed reduction of Ca^{2+} transfer from SR/ER to mitochondria was not the consequence of a diminution of the driving force between the two organelles.

Inhibition of GSK3β at reoxygenation limits both cytosolic and mitochondrial Ca^{2+} overload by reducing Ca^{2+} release from SR/ER. It has been previously demonstrated that inhibition of GSK3β at reperfusion is cardioprotective by preventing PTP opening.[6,7] However, the relative cardioprotective mechanism still remains unknown. We here hypothesized that this beneficial effect might be linked to the limitation of both cytosolic and mitochondrial Ca^{2+} overload (and subsequent Ca^{2+}-dependent PTP opening) by reducing Ca^{2+} release from IP_3R at reperfusion.

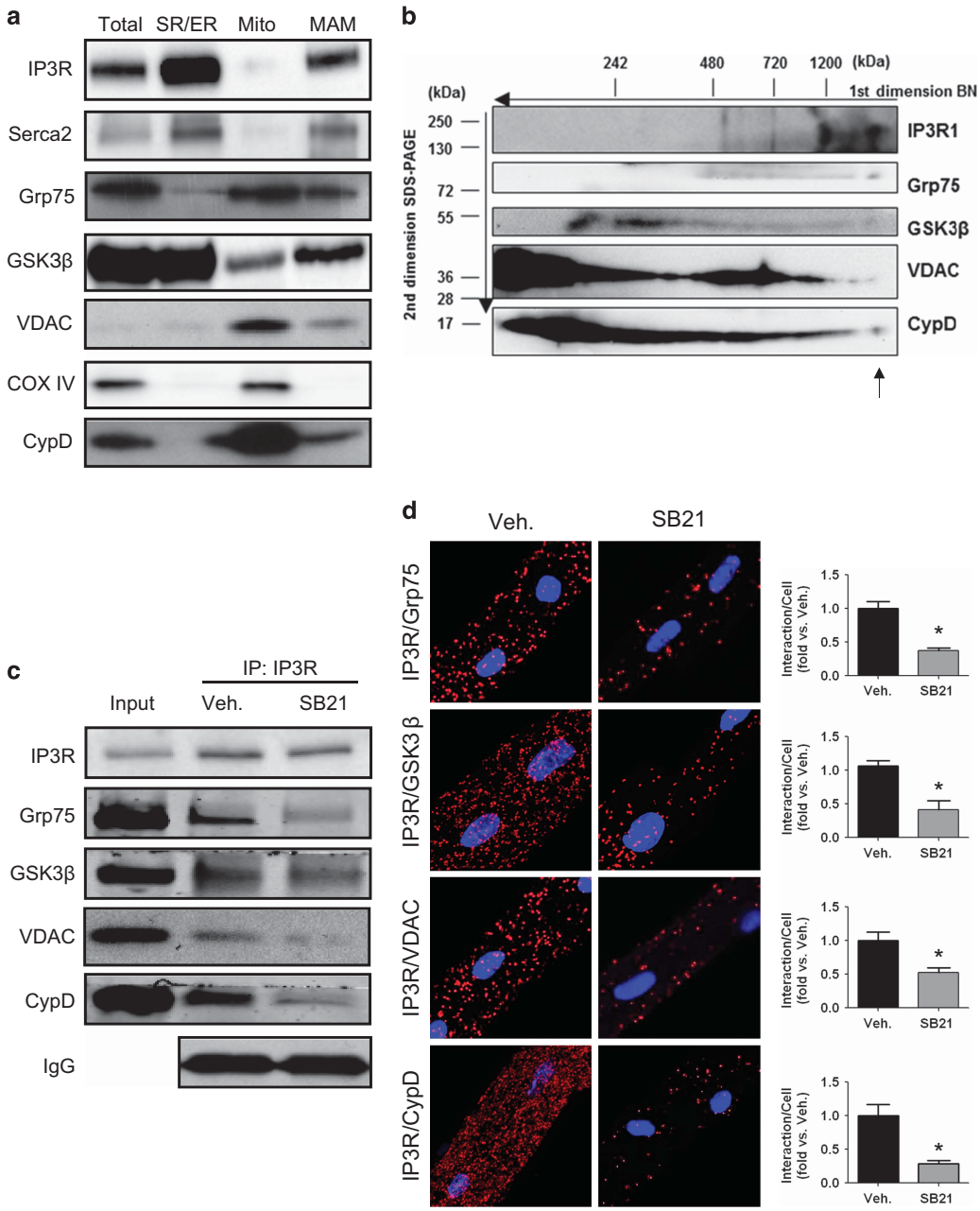

Figure 1 GSK3β modulates the IP_3R-Ca^{2+} channeling complex at MAMs in the heart. (**a**) Protein components of subcellular fractions prepared from WT mouse hearts revealed the presence of GSK3β in MAMs. Total, total heart homogenate; Mito, pure mitochondria; MAM, mitochondria-associated ER membranes. IP_3R and SERCA2 were used as cardiac SR/ER biomarkers. VDAC, Grp75, COXIV and CypD were used as mitochondrial biomarkers. (**b**) Two-dimensional blue native protein separation of WT heart homogenates. GSK3β was clearly detected in a high molecular weight complex encompassing IP_3R, Grp75, VDAC and CypD (arrow). (**c**) IP revealed that SB21 (a potent GSK3β inhibitor, 70 μg/kg) reduced the interaction of IP_3R with Grp75, GSK3β, VDAC and CypD in mice hearts (one representative out of $n=3$ is shown). (**d**) Typical images of *in situ* interactions between IP_3R with Grp75, GSK3β, VDAC and CypD using PLA in adult cardiomyocytes with or without SB21 treatment (6 μM). Quantification of the PLA red fluorescent dots was performed using BlobFinder V.3.2 and nuclei were stained in blue with 4',6-diamidino-2-phenylindole (DAPI). Indicated results are means $\pm$ S.E.M. of three distinct experiments (each experiment represents the average of 8–10 adult cardiomyocytes). *$P<0.05$ *versus* vehicle (Veh)

To test our hypothesis, we started by investigating reticular (ER), cytosolic and mitochondrial Ca^{2+} homeostasis after hypoxia reoxygenation (HR) in H9c2 cells. In the control group (HR), 4 h hypoxia followed by 2 h reoxygenation induced a significant cell death averaging $50.4\pm2.9\%$ *versus* $7.4\pm0.5\%$ in basal group; $P<0.05$ (Figure 3a). As expected, SB21 (6 μM) at reoxygenation significantly reduced the cell death by half-averaging $25.9\pm1.8\%$ *versus* $50.4\pm2.9\%$ in the HR group (Figure 3a).

The ER Ca^{2+} level (measured with D1ER sensor[24]) was significantly higher in cells treated with SB21 at reoxygenation averaging 2.19 ± 0.10 *versus* 1.44 ± 0.11 in the HR group (Figure 3b). After addition of thapsigargin, the efflux of ER Ca^{2+} was 2.5-fold higher in the HR+SB21 group compared

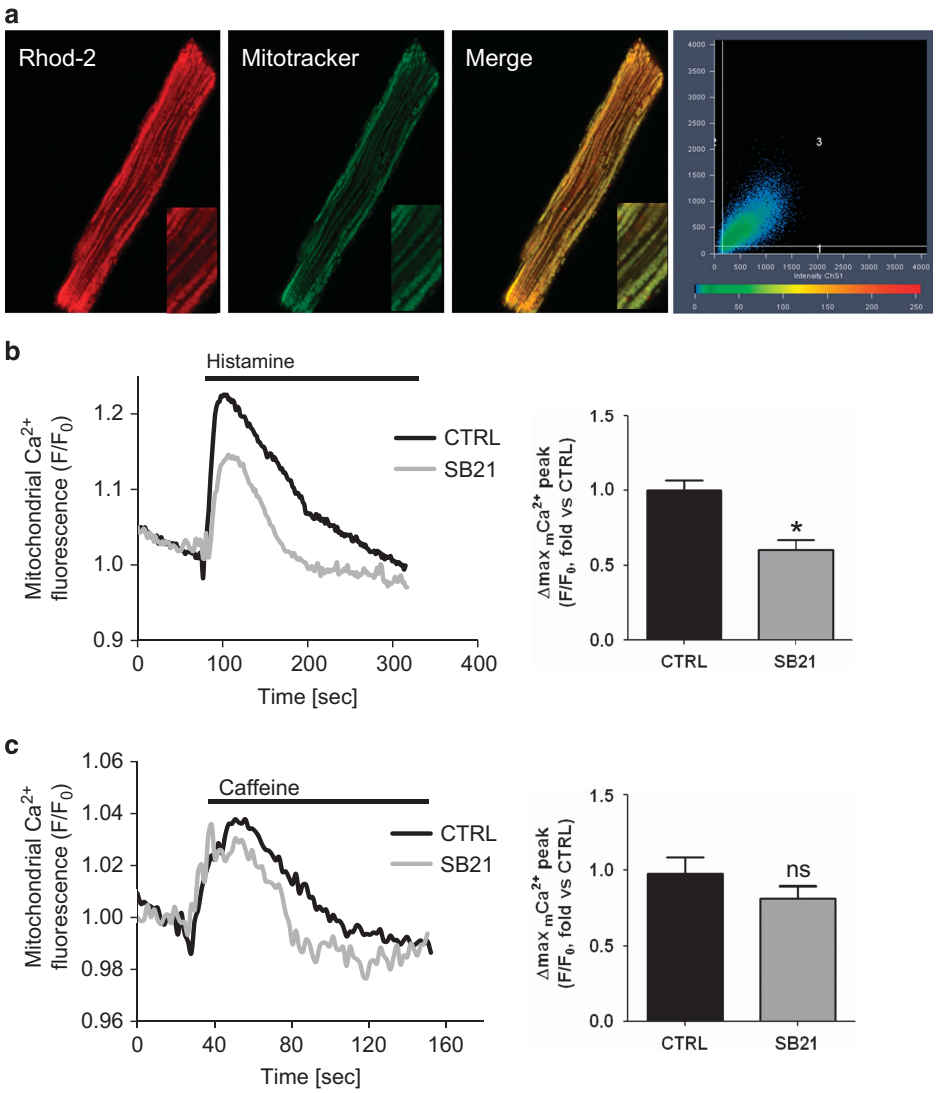

Figure 2 GSK3β regulates the SR/ER-mitochondria Ca^{2+} transfer through IP_3R in adult cardiomyocytes. (**a**) Adult cardiomyocytes were loaded with the Ca^{2+} indicator rhod-2 and MitoTracker Green. Merge signal revealed a mitochondrial pattern, especially apparent in enlarged insets. (Right) The quantitative pixel-by-pixel analysis measured with Zen software showed strong correlation between rhod-2 and Mitotracker Green with an overlap coefficient averaging 0.89 ± 0.01. (**b**) Representative traces of mitochondrial Ca^{2+} transients. Adult cardiomyocytes were challenged with 100 μM histamine to induce Ca^{2+} release from the ER. Mitochondrial Ca^{2+} transfer was significantly reduced under GSK3β inhibition (SB21). (**c**) Time scan of mitochondrial Ca^{2+} challenged with caffeine stimulation (5 mM) showed that inhibition of GSK3β did not modify the caffeine-induced Ca^{2+} transfer from SR/ER to mitochondria. Maximal mitochondrial Ca^{2+} peak fluorescence are expressed as means $\pm$ S.E.M. $^*P<0.05$ *versus* respective control ($n=5$–6 distinct experiments; each experiment represents the average of 8–12 adult cardiomyocytes)

with the HR group (Figure 3b), reinforcing the notion that inhibition of GSK3β at reoxygenation increases the steady-state $[Ca^{2+}]$ in ER lumen during HR.

As a consequence, the basal cytosolic Ca^{2+} measured with the ratiometric dye fura-2 was significantly reduced in the HR+SB21 group averaging 0.30 ± 0.02 *versus* 0.38 ± 0.01 in the HR group; $P<0.05$ (Figure 3c), and the IP_3R-mediated Ca^{2+} transfer from SR/ER to mitochondria was significantly abolished when GSK3β was inhibited at reoxygenation averaging 1.05 ± 0.02 *versus* 1.10 ± 0.03 in the HR group; $P<0.05$ (Figure 3d). Altogether, these results indicate that SB21-dependent cell protection is associated with a limitation of both cytosolic and mitochondrial Ca^{2+} overload likely through a reduction of Ca^{2+} release from SR/ER at reoxygenation.

IP_3R is a downstream substrate of GSK3β during IR injury. We then sought to determine the mechanism by which GSK3β regulates IP_3R in the heart. As IP_3Rs are known to contain the GSK3β consensus sequence (Ser/Thr-XXX-pSer/Thr) for phosphorylation (at Ser_{1756}) that activates IP_3R, we next questioned whether IP_3R might be phosphorylated by GSK3β at the SR/ER-mitochondria interface in the heart. To test this hypothesis, we investigated the posttranslational modification of IP_3R in adult cardiomyocytes during HR.

As expected, HR induced a significant cell death averaging $65.3 \pm 3.2\%$ *versus* $13.6 \pm 0.7\%$ in the basal group (Figure 4a). Concomitantly, we observed a significant increase in phosphorylation of GSK3β at tyrosine 216 (Tyr_{216}) residue (known to facilitate GSK3β activity) averaging 1.82 ± 0.08-

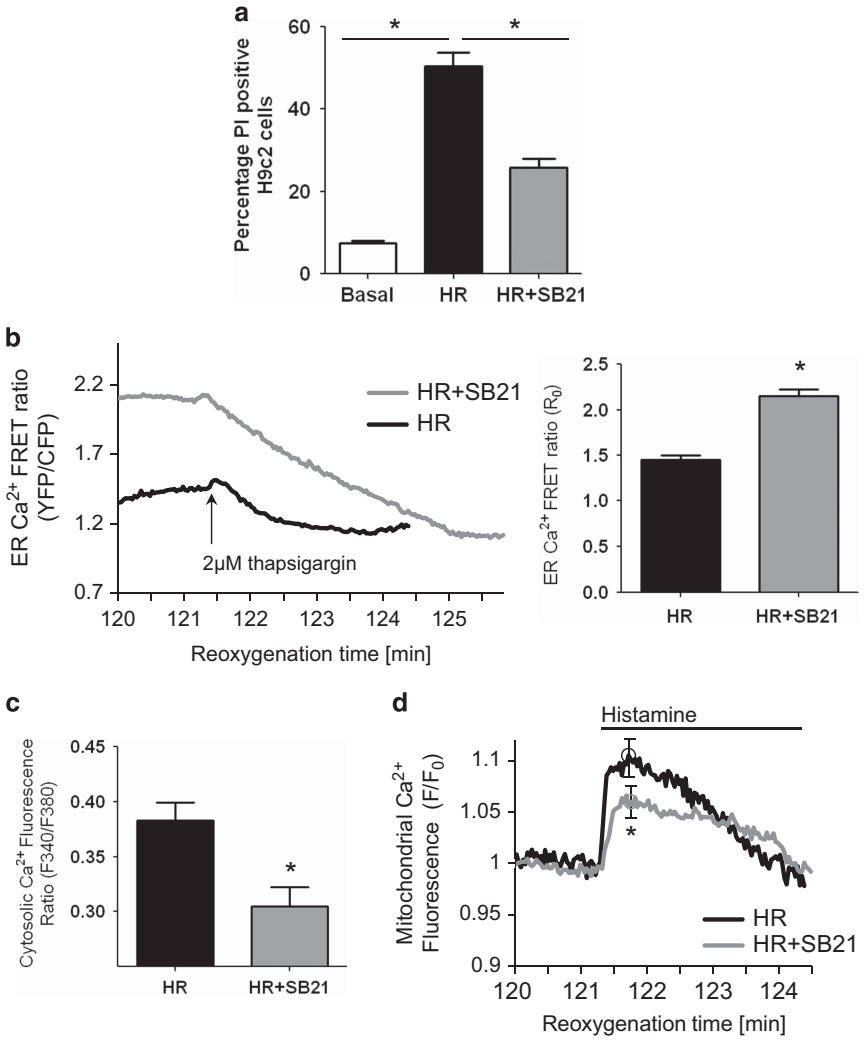

Figure 3 GSK3β regulates the SR/ER Ca^{2+} homeostasis at reoxygenation in H9c2 cells. (**a**) Cell viability measured with propidium iodide revealed that SB21 clearly protected H9c2 cells against reoxygenation injury. Bar graphs were presented as the mean ± S.E.M. ($n = 4$ distinct experiments per group). *$P < 0.05$. (**b**) Representative curves of SR/ER Ca^{2+} FRET ratio in hypoxic H9c2 cells. After 2 h reoxygenation, ER Ca^{2+} level was significantly higher in cells treated with SB21 (6 μM) at reoxygenation. Indicated results are means ± S.E.M. of 4–6 distinct experiments (each experiment represents the average of 6–8 H9c2 cells). The addition of thapsigargin (2 μM) induced an ER Ca^{2+} efflux, which was 2.5-fold higher in the HR+SB21 group compared with the HR group (arrow). (**c**) Measurement of cytosolic Ca^{2+} at the end of reoxygenation with fura-2 (5 μM) with or without SB21 (6 μM). Results are means ± S.E.M. of 4–5 distinct experiments. (Each experiment represents the average of 20–30 H9c2 cells.) *$P < 0.05$ *versus* HR. (**d**) Representative curves of the time scan of mitochondrial Ca^{2+} (rhod-2, 2.5 μM) upon histamine stimulation (100 μM) after HR with or without SB21 at reoxygenation. Peak mitochondrial Ca^{2+} amplitude is expressed as means ± S.E.M. *$P < 0.05$ *versus* HR ($n = 5$–6 distinct experiments; each experiment represents the average of 8–12 H9c2 cells)

versus 1.00 ± 0.05-fold in the basal group; $P < 0.05$ (Figure 4b). At reoxygenation, SB21 significantly reduced both cell death (around 50%; Figure 4a) and phosphorylation at Tyr_{216} of GSK3β averaging 1.18 ± 0.10 *versus* 1.82 ± 0.08 in the HR group (Figure 4b). These results suggest that GSK3β activity is linked with cell death of adult cardiomyocytes during HR.

HR induced a significant increase of IP_3R phosphorylation of Ser_{1756}, which was markedly reduced by SB21 at reoxygenation averaging 6.24 ± 0.42- and 1.32 ± 0.12-fold *versus* basal, respectively (Figure 4c). The decreased IP_3R phosphorylation and the consecutive limitation of its activity seem to be an important mechanism in the protection of cardiomyocytes elicited by GSK3β inhibition at reoxygenation. This idea was supported by the protein–protein interaction of GSK3β with IP_3R in cardiomyocytes during HR. Indeed, using the PLA approach, our data showed that HR doubled the interaction of GSK3β with IP_3R averaging 2.23 ± 0.23- *versus* 1.0 ± 0.19-fold in basal (Figure 4d). SB21 reduced this interaction at reoxygenation averaging 0.74 ± 0.10 *versus* 2.23 ± 0.23 in the HR group ($P < 0.05$, Figure 4d), suggesting that IP_3R might be a downstream substrate of GSK3β during HR injury.

Eventually, we tested whether GSK3β regulates the post-translational modification of IP_3R during *in vivo* IR injury in a mouse model. As previously demonstrated by our group,[6,7] mice treated with SB21 at reperfusion (IR+SB21, 70 μg/kg) exhibit a significant reduction of infarct size after prolonged IR injury when compared with control (IR), averaging 31.0 ± 0.6% *versus* 44.6 ± 1.7%, respectively (Figure 5a). SB21 administered at reperfusion significantly decreased the phosphorylation of both GSK3β (Tyr_{216}) and IP_3R (Ser_{1756}) induced by reperfusion injury (Figures 5b and c), suggesting that GSK3β controls the extent of infarct size through the regulation of the

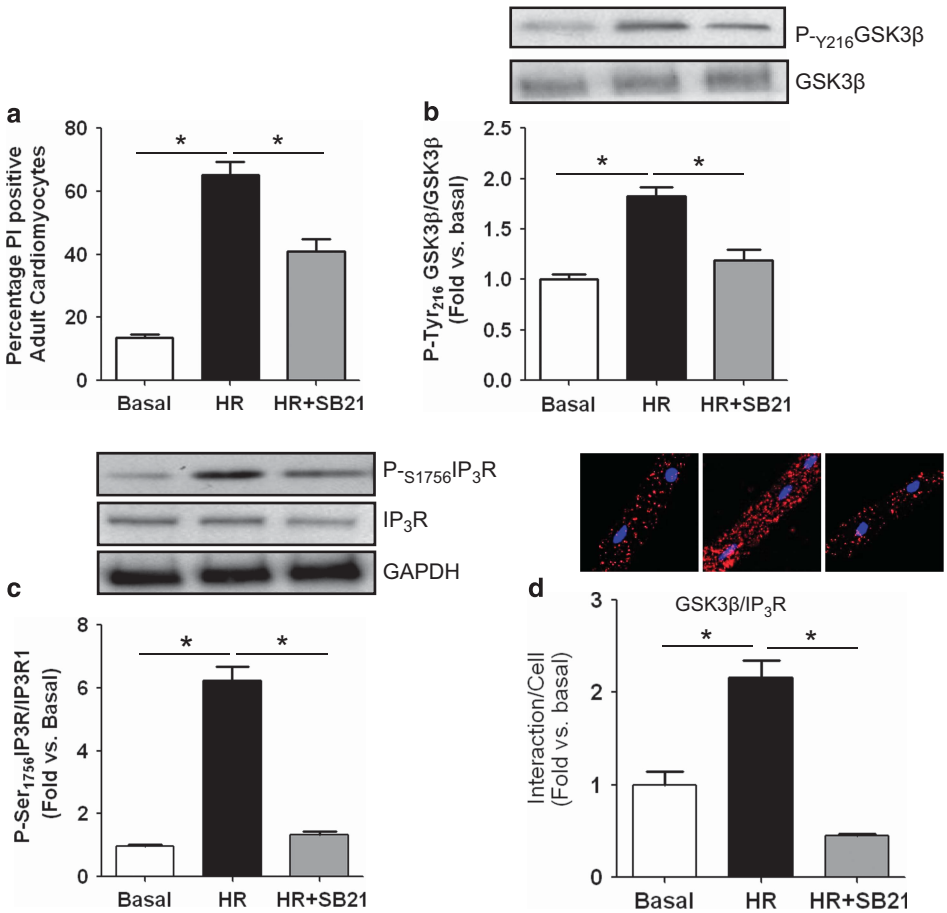

Figure 4 GSK3β inhibition at reoxygenation reverses the activation of IP_3R induced by HR in adult cardiomyocytes. (**a**) Cell viability measured with propidium iodide revealed that SB21 clearly protected adult cardiomyocytes against reoxygenation injury ($n=4$ distinct experiments per group); mean ± S.E.M. of cell death is shown as percentage. *$P<0.05$. (**b**) GSK3β activity quantified by western immunoblotting of phospho-GSK3β (Tyr_{216}, active form) under hypoxic conditions. Results were normalized with total GSK3β ($n=4$–5 distinct experiments per group). *$P<0.05$. (**c**) Immunoblotting of relative expression of phosphor-Ser_{1756} IP_3R normalized with total IP_3R during HR injury. Results expressed as fold *versus* basal are means ± S.E.M. *$P<0.05$ ($n=4$ distinct experiments). (**d**) *In situ* protein interactions using PLA in adult cardiomyocytes revealed that SB21 (6 μM) significantly reduced the interaction of GSK3β with IP_3R induced by HR. Results are expressed as means ± S.E.M. of 8–10 distinct experiments (each experiments represent the average of 4–8 adult cardiomyocytes). *$P<0.05$

phosphorylation state of IP_3R at reperfusion. The *in vivo* link between GSK3β and IP_3R was further reinforced by the reduction of IP_3R co-IP with the partner of the Ca^{2+} channeling complex at MAMs including GSK3β, as well as Grp75, VDAC and CypD in the area at risk of ischemic hearts treated with SB21 at reperfusion (Figure 5d).

Discussion

The present results suggest that (1) a fraction of GSK3β is localized at the SR/ER-mitochondria interface in the heart; (2) GSK3β regulates the IP_3R-dependent Ca^{2+} transfer from SR/ER to mitochondria in cardiac cells and (3) cardioprotection mediated by GSK3β inhibition limits both cytosolic and mitochondrial Ca^{2+} overload by limiting IP_3R channel opening at reperfusion.

We examined whether inhibition of GSK3β might protect the heart from reperfusion injury.[7] Our results point to a regulatory effect of GSK3β on the Ca^{2+} transfer between SR/ER and mitochondria at the MAMs interface during IR injury.

In the heart, although a mitochondrial targeting sequence (MTS) has not been identified in GSK3β, it has been recently demonstrated that an N-terminal domain of GSK3β could function as an MTS, permitting the translocation of GSK3β to mitochondria in a kinase-activity-dependent manner to regulate mitochondrial functions.[13] Here, we show that a fraction of GSK3β is located in SR/ER and MAMs. We demonstrated that GSK3β physically interacts with the IP_3R-Ca^{2+} channeling complex including VDAC, Grp75, CypD and IP_3R at MAMs. Moreover, we found that pharmacological and siRNA-mediated inhibition of GSK3β altered the interaction among proteins of the IP_3R-Ca^{2+} channeling complex, suggesting a role for GSK3β in the structure of this complex.

We observed that GSK3β does not interact with RyRs, and the RyR-dependent Ca^{2+} release does not seem to be affected by GSK3β inhibition in cardiac cells. The inhibition of GSK3β was sufficient to reduce the Ca^{2+} transfer from SR/ER to mitochondria via a specific action on IP_3R Ca^{2+} leak channels at MAMs. One can therefore question the respective importance of IP_3Rs- *versus* RyRs-mediated Ca^{2+} release following reperfusion injury in cardiomyocytes. IP_3Rs are

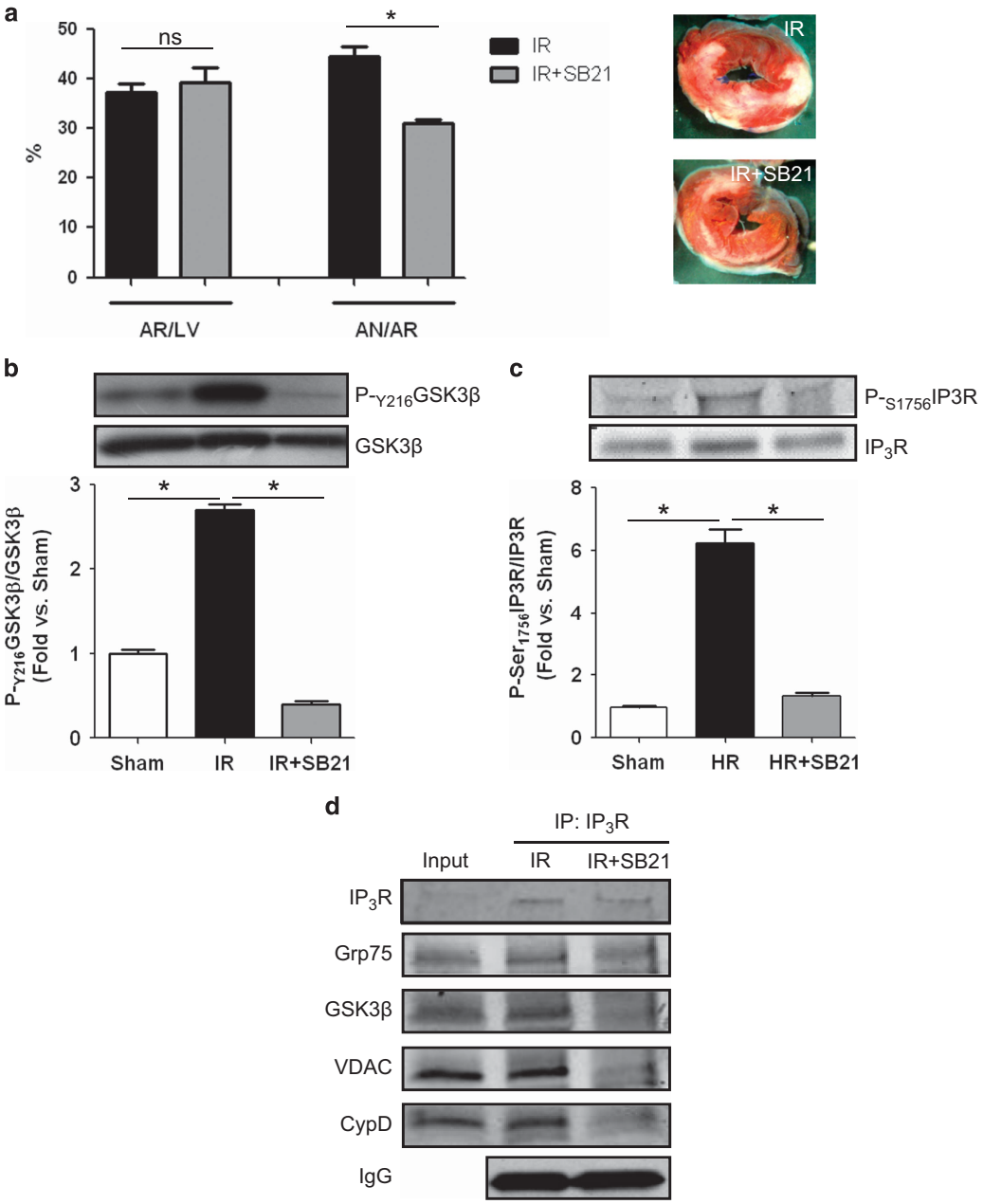

Figure 5 *In vivo* GSK3β inhibition-mediated cardioprotection is correlated to the inactivation of IP_3R at reperfusion. (**a**) Cardioprotective effect of SB21 at reperfusion. Percentage of both area at risk (AR/LV) and area of necrosis (AN/AR) are presented for each groups ($n=6$ per group). As illustrated in the right panel, injection of SB21 (70 μg/kg) at reperfusion reduced the size of myocardial infarction compared with IR group. (**b**) Relative GSK3β activity at reperfusion quantified by western immunoblotting of phospho-GSK3β (Tyr_{216}, active form). Results were normalized with total GSK3β ($n=4$–5 distinct experiments per group). *$P<0.05$. (**c**) Immunoblotting of relative expression of phospho-Ser_{1756} IP_3R revealed that SB21 significantly reduced the activity of IP_3R during IR injury. Results are means $\pm$ S.E.M. *$P<0.05$ ($n=4$–6 distinct experiments). (**d**) Hearts protected with SB21 (70 μg/kg) at reperfusion exhibited a clear reduction of IP_3R interaction with Grp75, GSK3β, VDAC and CypD. Results shown are one result representative of three trials

involved in cardiac Ca^{2+} signaling including the ECC in the normal heart, and also in some pathologies such as hypertrophy.[19,25–27] Our data reinforce this idea as both pharmacologic and genetic inhibition of GSK3β leads to a decreased Ca^{2+} transfer from SR/ER to mitochondria, whereas overexpression of GSK3β enhances the entrance of Ca^{2+} into mitochondria under IP_3R leak channel stimulation.

Whether GSK3β inhibition specifically impacts the SR/ER Ca^{2+}release or rather the Ca^{2+} entrance into mitochondria was not addressed in this study. Nevertheless, we demonstrated that pharmacological or genetic inhibition of GSK3β did not modify the mitochondrial membrane potential, indicating that the observed reduction of Ca^{2+} transfer from SR/ER to mitochondria was likely not the result of a limitation of the driving force between the two organelles.

Upon IR, the accumulation of Ca^{2+} into mitochondria is known to trigger PTP opening and cell death.[28] Ca^{2+} crosstalk

between SR/ER and mitochondria has been involved in myocardial reperfusion injury.[29] As cardioprotective mechanisms of GSK3β at reperfusion are still not clear, we hypothesized that GSK3β inhibition limits both cytosolic and mitochondrial Ca^{2+} overload by limiting IP_3R channel opening and subsequent PTP-dependent cell death at reperfusion.

We demonstrated here that the interaction of GSK3β with all the partners of IP_3R Ca^{2+} channeling complex, including CypD, VDAC, Grp75 and IP_3R, was significantly increased after HR and associated with mitochondrial Ca^{2+} overload and cell death. Interestingly, the pharmacological inhibition of GSK3β not only decreased the interaction of GSK3β with the Ca^{2+} channeling complex but also decreased the protein composition of the IP_3R channeling complex and attenuated both cytosolic and mitochondrial Ca^{2+} overload at reperfusion. This suggests that binding of GSK3β to IP_3R may be responsible of the Ca^{2+} crosstalk between SR/ER and mitochondria during reperfusion injury.

Different observations were in favor of the causal connection of GSK3β with IP_3R during IR. First, we provide *in vivo* and *in vitro* evidence that pharmacological inhibition of GSK3β reduced the physical interaction of GSK3β with IP_3R induced by IR. Second, the Ser_{1756} phosphorylation of IP_3R was significantly reduced when GSK3β was inhibited at reperfusion. As a result, the open probability of the Ca^{2+} channels was reduced at reperfusion inducing a higher level of Ca^{2+} into SR/ER lumen and a reduction of Ca^{2+} overload in both cytosol and mitochondria. Third, GSK3β inhibition at reperfusion reduced the interaction of IP_3R with the other partners of the Ca^{2+} channeling complex including CypD, VDAC, Grp75 and GSK3β.

Although IP_3R2 is recognized as the predominant isoform in the cardiac myocyte,[27] IP_3R1 is highly expressed in MAMs heart.[21,30,31] Our results show that GSK3β preferentially interacts with IP_3R1, and can also interacts with IP_3R2 and IP_3R3 in cardiac cells (data not shown). In summary, we propose that inhibition of GSK3β might decrease the phosphorylation and the activity of IP_3R, thereby limiting cytosolic and mitochondrial Ca^{2+} overload, possibly contributing to the reduction of both cell death and infarct size at reperfusion. Our proposal is in line with previous reports demonstrating that SR/ER loses almost 90% of its Ca^{2+} at the onset of reperfusion,[32] and that specific IP_3R channels inhibition can protect the heart at reperfusion.[33] One may question whether IP_3R may be a direct or an indirect substrate of GSK3β. Such mechanism remains to be investigated in-depth in future studies. However, our results showed (1) a positive correlation between the activity of GSK3β and the phosphorylation rate of IP_3R, (2) a linear correlation between the Ser_{1756} phosphorylation of IP_3R and the protein–protein interaction of GSK3β with IP_3R and (3) *in silico* analysis revealed at least two putative GSK3β phosphorylation sites on IP_3R, Ser_{1756} and Ser_{1765}, reinforcing the notion that IP_3R could be a substrate of GSK3β.

Whether other factors may contribute to the increase of Ca^{2+} into SR/ER lumen upon inhibition of GSK3β at reperfusion remains to be determined (i.e. ANT, VDAC, CypD). Moreover, we cannot fully exclude a contribution of SERCA2 since Michael *et al.*[12] previously demonstrated that overexpression of GSK3β could significantly reduce the expression of SERCA2 in the heart.[12] We noticed in the present work that SERCA2 expression seems to be increased when GSK3β was inhibited at the onset of reperfusion (data not shown). Such mechanism remains to be investigated in-depth in future studies, especially since a problem of timing has to be considered between the speed of Ca^{2+} response and the time needed for SERCA2 protein transcription at the onset of reperfusion.

To conclude, our work identifies a new role for GSK3β in cardioprotection as an important regulator of Ca^{2+} transfer between SR/ER and mitochondria during IR injury. We propose that GSK3β inhibition at reperfusion may protect heart through the limitation of SR/ER Ca^{2+} release by inhibition of IP_3R Ca^{2+} channeling complex and consecutive reduction of both cytosolic and mitochondrial Ca^{2+} overload and subsequent PTP opening.

Materials and Methods

Animals. The investigation conformed to the *Guide for the Care and Use of Laboratory Animals* published by the US National Institute of Health (NIH Publication No. 85-23, revised 1996) and was approved by the local institutional animal research committee (N BH2012-64 and 901l).

Subcellular fractionation. Cell fractionation was performed by differential ultracentrifugation as described previously.[22,34] Briefly, hearts were homogenized with a glass potter in an isolation buffer (225 mM mannitol, 75 mM sucrose, 0.5% BSA, 0.5 mM EGTA and 30 mM Tris-HCl, pH 7.4). Both nuclei and cellular debris were then pelleted by two different centrifugations at 740 × *g* for 5 min. The supernatant was centrifuged at 9000 × *g* for 10 min to pellet crude mitochondria that were resuspended in mitochondria resuspending buffer (MRB) containing 250 mM mannitol, 5 mM HEPES and 0.5 mM EGTA, pH 7.4. Resulting supernatant was further centrifuged at 20 000 × *g* for 30 min followed by 100 000 × *g* for 1 h to pellet the SR/ER.

Purified mitochondria were obtained by centrifugation of crude mitochondria fraction through a Percoll medium at 95 000 × *g* for 30 min in an SW40 rotor (Beckman Coulter, Villepinte, France). The resulting pellet was then washed two times in MRB by centrifugation at 6300 × *g* for 10 min to obtain purified mitochondria.

To purify the MAM fraction localized in the diffused white band (under pure mitochondria band), MAM were diluted in MRB and centrifuged at 6300 × *g* for 10 min to remove any contaminating mitochondria. MAM supernatant was then centrifuged at 100 000 × *g* for 1 h in a 70 Ti rotor (Beckman Coulter) and the resulting pellet was resuspended in MRB. Protein content was assayed by the Lowry method for the following analysis.

Blue native and SDS-PAGE 2D separation. Hearts from wild-type (WT) mice were homogenized three times at 6000 Hz for 10 s (Precellys 24; Ozyme, Montigny-le-Bretonneux, France) in a buffer (100 mM KCl, 50 mM MOPS, 5 mM $MgSO_4$, 1 mM EGTA, 1 mM ATP). Heart homogenates were then solubilized with *n*-dodecyl-β-D-maltopyranoside (detergent/protein ratio of 1.6:1, g/g), combined with Coomassie Blue G-250 dye (detergent/dye ratio of 4:1, g/g) and separated on 4–16% Bis-Tris native PAGE gels (Invitrogen, Cergy Pontoise, France) for the first dimension. The first dimension gel was then excised and reduced with 1 × NuPage reducing agent in 1 × NuPage LDS sample buffer (Invitrogen) for 15 min at room temperature (RT). Cysteine alkylation was carried out with *N*, *N*-dimethylacrylamide for 15 min at RT. The reaction was quenched for 15 min at RT with 20% ethanol in 1 × LDS and 0.1 × reducing agent. Finally, the equilibrated gel strip was applied to the second dimension on a 4–16% Criterion Bis-Tris gel, separated and transferred to the PVDF membrane.

IP and WB analysis. Total lysates of cardiac cells were prepared in lysis buffer containing 1% NP40, 20 mM Tris-HCl, 138 mM NaCl, 2.7 mM KCl, 1 mM $MgCl_2$, 5% glycerol, 5 mM EDTA, 1 mM DTT supplemented with a cocktail of protease inhibitors (Sigma-Aldrich, Saint-Quentin Fallavier, France) and phosphatases inhibitors (PhosphoStop; Roche Diagnostics, Meylan, France). For IP, 2 μg of antibodies directed against the protein of interest were added to the IP buffer (except for the control, which was supplemented with 2 μg of anti-mouse IgG).

A range of 300–500 μg of total protein (depending on the origin of the samples) was added in the previous mix and incubated overnight at 4 °C. Fifty microliters of magnetic beads (Millipore, Fontenay sous Bois, France; no. LSKMAGG10) were then incubated for 2 h at 4 °C and finally precipitated with a strong magnet. After three washes in IP buffer, proteins were resuspended in Laemmli buffer and denatured at 95 °C for 10 min. Immunoprecipitated proteins were then analyzed by WB. Migration was performed in 4–20% acrylamide gel and semidry blotter was used to transfer the proteins. All primary antibodies were used at a dilution of 1:1000, except CypD (1 : 4000). Mouse and rabbit secondary antibodies were incubated for 1 h at RT at 1 : 10 000 (Bio-Rad, Marnes-la-Coquette, France). ECL+ reagent (GE Healthcare, Velizy-Villacoublay, France) was used for the membrane revelation, acquisition was performed with Bio-Rad Molecular Imager Gel Doc XR+, and ImageLab software was used for quantification (Bio-Rad). Antibodies IP3R (sc-28614), Grp75 (sc133137), P-GSK3β (sc-135653) and IgG (sc-66931) were from Santa Cruz Biotechnology (Dallas, TX, USA); P-IP3R (no. 8548), GSK3β (no. 9315), Serca2 (no. 4388), COXIV (cs no. 4844) and GAPDH (no. 2118) were from Cell Signaling Technology (Saint Quentin Yvelines, France); and VDAC (Ab14734), CypD (Ab110324) and RyR2 (Ab 117840) were from Abcam (Paris, France). Relative expressions of phosphorylated proteins were normalized to respective total form and results were expressed as fold *versus* basal condition.

Isolation of adult murine cardiomyocytes. Ventricular cardiomyocytes were isolated using enzymatic digestion according to previously described procedure.[35,36] Briefly, WT mice were anesthetized with pentobarbital (70 mg/kg) (Sanofi Santé Animale, Libourne, France) and the heart was quickly harvested and retrogradely perfused at 37 °C for 6–8 min with a perfusion buffer (113 mM NaCl, 4.7 mM KCl, 0.6 mM KH_2PO_4, 0.6 mM Na_2HPO_4, 1.2 mM $MgSO_4$, 12 mM $NaHCO_3$, 10 mM $KHCO_3$, 10 mM HEPES, 30 mM Taurine, pH 7.4) containing 10 mM 2,3-butanedione, 5.5 mM glucose, 12.5 μM $CaCl_2$, 0.1 mg/ml of liberase (Roche) and 0.14 mg/ml trypsin (Sigma). Isolated myocytes were then maintained in culture in laminin- (10 μg/ml) precoated dishes with M199 medium (Invitrogen) and allowed to attach for 2 h before analysis.

Duolink *in situ* PLA. We used PLA experiments to evaluate the proximity of two proteins and their potential interaction (<40 nm) as described previously.[22] Adult cardiomyocytes (or H9c2 cells) were plated into Lab-Tech slides (Thermo Scientific; no.155411). Cells were first fixed in 4% PFA for 10 min at RT. Cell permeabilization was carried out in 0.1% Triton X-100 for 15 min at RT followed by blocking for 30 min in a 37 °C preheated humidity chamber. Primary antibodies directed against the two proteins of interest were then added at 1 : 200 and incubated overnight at 4 °C. From this point, each step was separated by two washes of 5 min in TBST and incubations were performed at 37 °C in a humidity chamber. PLA probes, which are composed of antibodies linked to small complementary oligonucleotides, were added in accordance with the polarity for 1 h. Ligation reaction was then performed for 30 min to ligate the complementary oligonucleotides. Polymerization of the ligated fragment was performed with a Taq polymerase (Duolink II *in situ* PLA; Olink Bioscience). Cells were then washed in 1 × and 0.01 × SSC buffer (150 mM NaCl, 15 mM sodium citrate for 1 ×) and dried at RT in the dark to preserve fluorescence. Slides were mounted in mounting medium containing DAPI and observed with a Leica SP5X confocal microscope (Wetzar, Germany). A maximum intensity projection created an output image from Z stack performed at 0.5 μm depth. A total of 10–15 cells were counted in each experiment ($n=7$–16) for quantification. We used BlobFinder software (Image Analysis, Uppsala University, Uppsala, Sweden) to quantify the red dots corresponding to the positive interaction of the different proteins of interest.

Cytosolic, mitochondrial and SR/ER Ca^{2+} measurements. To monitor mitochondrial Ca^{2+}, isolated adult cardiomyocytes (or H9c2 cells) were loaded with 2.5 μM rhod-2/AM (Molecular Probes, Eugene, OR, USA) for 30 min at 37 °C in the presence of 0.003% (w/v) pluronic acid. After 5 h de-esterification, cardiac cells were washed and placed in 1 ml phenol-free DMEM to the heated stage (37 °C) of an inverted epifluorescence microscope (x40 oil-immersion objective) connected to a cooled CCD camera (PXL; Photometrics). Cytosolic Ca^{2+} dynamics were measured on H9c2 loaded with 5μM fura-2/AM. Imaging was performed with a digital cooled CCD camera (Photometrics, Tucson, AZ, USA) on an inverted microscope (Nikon Diaphot, Melville, NY, USA) using a x40 oil-immersion objective. SR/ER Ca^{2+} level was measured with a FRET-based genetic sensor (D1ER), which allows quantification of Ca^{2+} because of its ratiometric properties.[37]

Cellular models of HR. Adult cardiomyocytes or H9c2 were subjected to simulated hypoxia in a controlled hypoxic chamber (Adelbio, Clermont-Ferrand, France), induced by nitrogen flushing up to 1% partial O_2 pressure for 45 min and 4 h, respectively, in a Tyrode solution (130 mM NaCl, 5 mM KCl, 10 mM HEPES, 1 mM $MgCl_2$, 1.8 mM $CaCl_2$ at pH 7.4/37 °C) followed by 2 h of reoxygenation at 37 °C in normal culture medium. Cells received vehicle with no additional intervention (HR) or 6 μM SB21 (HR+SB21) at the onset of reoxygenation. Time control group consisted of cells without the hypoxic stimulus. Cell death was measured by counting PI-positive cells by imaging or flow cytometry (FACSCalibur; BD Biosciences, Le Pont de Claix, France) at the end of the reperfusion period.

***In vivo* model of acute myocardial IR injury.** C57BL/6 J (male, 8–10 weeks old) were anesthetized by intraperitoneal mixture of 70 mg/kg pentobarbital sodium and 0.1 mg/kg buprenorphine as described previously.[7,38–40] The animals were orally intubated, ventilated and body temperature was maintained at 37 °C. A left thoracotomy was performed in the fourth intercostal space. A small curved needle was passed around the left anterior descending coronary artery to induce IR. Mice were subjected to 45 min regional myocardial ischemia followed by 24 h reperfusion. Myocardial infarct size was then determined by triphenyltetrazolium staining as described previously.[7,38–40]

Statistical analysis. Data are presented as mean $\pm$ S.E.M., unless otherwise specified. Statistical analysis was performed with GraphPad Prism 5 software (La Jolla, CA, USA) with the use of nonparametric tests. Comparisons among >2 groups were analyzed by the Kruskal–Wallis test. When the Kruskal–Wallis test was significant, the Dunn's appropriate multiple testing procedure was performed. For all other analysis, data were compared by the Mann–Whitney rank-sum test. Statistical significance was defined as a value of $P<0.05$.

Conflict of Interest

The authors declare no conflict of interest.

Acknowledgements. LG was supported by French Grant EXPLORA'PRO 2013. We thank Prof. Dr. Roger Tsien for D1ER plasmid, the MitoCare center (Thomas Jefferson University Philadelphia, Philadelphia, PA, USA) and the CeCile Imaging Center (Lyon, France) for their assistance and advices in imaging analysis. We extend our thanks to Steve Hurst for his careful review of the manuscript.

1. Embi N, Rylatt DB, Cohen P. Glycogen synthase kinase-3 from rabbit skeletal muscle. Separation from cyclic-amp-dependent protein kinase and phosphorylase kinase. *Eur J Biochem* 1980; **107**: 519–527.
2. Woodgett JR, Cohen P. Multisite phosphorylation of glycogen synthase. Molecular basis for the substrate specificity of glycogen synthase kinase-3 and casein kinase-ii (glycogen synthase kinase-5). *Biochim Biophys Acta* 1984; **788**: 339–347.
3. Woodgett JR. Molecular cloning and expression of glycogen synthase kinase-3/factor a. *EMBO J* 1990; **9**: 2431–2438.
4. Cross DA, Alessi DR, Cohen P, Andjelkovich M, Hemmings BA. Inhibition of glycogen synthase kinase-3 by insulin mediated by protein kinase b. *Nature* 1995; **378**: 785–789.
5. Antos CL, McKinsey TA, Frey N, Kutschke W, McAnally J, Shelton JM *et al.* Activated glycogen synthase-3beta suppresses cardiac hypertrophy in vivo 10.1073/pnas.231619298. *Proc Natl Acad Sci USA* 2002; **99**: 907–912.
6. Tong H, Imahashi K, Steenbergen C, Murphy E. Phosphorylation of glycogen synthase kinase-3beta during preconditioning through a phosphatidylinositol-3-kinase-dependent pathway is cardioprotective. *Circ Res* 2002; **90**: 377–379.
7. Gomez L, Paillard M, Thibault H, Derumeaux G, Ovize M. Inhibition of gsk3beta by postconditioning is required to prevent opening of the mitochondrial permeability transition pore during reperfusion. *Circulation* 2008; **117**: 2761–2768.
8. Juhaszova M, Zorov DB, Kim SH, Pepe S, Fu Q, Fishbein KW *et al.* Glycogen synthase kinase-3beta mediates convergence of protection signaling to inhibit the mitochondrial permeability transition pore. *J Clin Invest* 2004; **113**: 1535–1549.
9. Nishihara M, Miura T, Miki T, Tanno M, Yano T, Naitoh K *et al.* Modulation of the mitochondrial permeability transition pore complex in gsk-3[beta]-mediated myocardial protection. *J Mol Cell Cardiol* 2007; **43**: 564–570.
10. Pastorino JG, Hoek JB, Shulga N. Activation of glycogen synthase kinase 3beta disrupts the binding of hexokinase ii to mitochondria by phosphorylating voltage-dependent anion channel and potentiates chemotherapy-induced cytotoxicity. *Cancer Res.* 2005; **65**: 10545–10554.
11. Rasola A, Sciacovelli M, Chiara F, Pantic B, Brusilow WS, Bernardi P. Activation of mitochondrial erk protects cancer cells from death through inhibition of the permeability transition. *Proc Natl Acad Sci USA* 2010; **107**: 726–731.

12. Michael A, Haq S, Chen X, Hsich E, Cui L, Walters B *et al.* Glycogen synthase kinase-3beta regulates growth, calcium homeostasis, and diastolic function in the heart. *J Biol Chem* 2004; **279**: 21383–21393.
13. Tanno M, Kuno A, Ishikawa S, Miki T, Kouzu H, Yano T *et al.* Translocation of glycogen synthase kinase-3beta (gsk-3beta), a trigger of permeability transition, is kinase activity-dependent and mediated by interaction with voltage-dependent anion channel 2 (vdac2). *J Biol Chem* 2014; **289**: 29285–29296.
14. Braunwald E, Kloner RA. Myocardial reperfusion: a double-edged sword? *J Clin Invest* 1985; **76**: 1713–1719.
15. Borgers M, Thone F, Van Reempts J, Verheyen F. The role of calcium in cellular dysfunction. *Am J Emerg Med.* 1983; **1**: 154–161.
16. Rizzuto R, Marchi S, Bonora M, Aguiari P, Bononi A, De Stefani D *et al.* Ca(2+) transfer from the ER to mitochondria: When, how and why. *Biochim Biophys Acta* 2009; **1787**: 1342–1351.
17. Bers DM. Cardiac excitation–contraction coupling. *Nature* 2002; **415**: 198–205.
18. Domenech RJ, Sanchez G, Donoso P, Parra V, Macho P. Effect of tachycardia on myocardial sarcoplasmic reticulum and Ca^{2+} dynamics: a mechanism for preconditioning? *J Mol Cell Cardiol* 2003; **35**: 1429–1437.
19. Signore S, Sorrentino A, Ferreira-Martins J, Kannappan R, Shafaie M, Del Ben F *et al.* Inositol 1, 4, 5-trisphosphate receptors and human left ventricular myocytes. *Circulation* 2013; **128**: 1286–1297.
20. Hayashi T, Su TP. Sigma-1 receptor chaperones at the er-mitochondrion interface regulate Ca(2+) signaling and cell survival. *Cell* 2007; **131**: 596–610.
21. Szabadkai G, Bianchi K, Varnai P, De Stefani D, Wieckowski MR, Cavagna D *et al.* Chaperone-mediated coupling of endoplasmic reticulum and mitochondrial Ca^{2+} channels. *J Cell Biol* 2006; **175**: 901–911.
22. Paillard M, Tubbs E, Thiebaut PA, Gomez L, Fauconnier J, Da Silva CC *et al.* Depressing mitochondria-reticulum interactions protects cardiomyocytes from lethal hypoxia–reoxygenation injury. *Circulation* 2013; **128**: 1555–1565.
23. Louch WE, Sheehan KA, Wolska BM. Methods in cardiomyocyte isolation, culture, and gene transfer. *J Mol Cell Cardiol* 2011; **51**: 288–298.
24. McCombs JE, Palmer AE. Measuring calcium dynamics in living cells with genetically encodable calcium indicators. *Methods* 2008; **46**: 152–159.
25. Kijima Y, Saito A, Jetton TL, Magnuson MA, Fleischer S. Different intracellular localization of inositol 1,4,5-trisphosphate and ryanodine receptors in cardiomyocytes. *J Biol Chem* 1993; **268**: 3499–3506.
26. Tuvia S, Buhusi M, Davis L, Reedy M, Bennett V. Ankyrin-b is required for intracellular sorting of structurally diverse Ca^{2+} homeostasis proteins. *J Cell Biol* 1999; **147**: 995–1008.
27. Vermassen E, Parys JB, Mauger JP. Subcellular distribution of the inositol 1,4,5-trisphosphate receptors: functional relevance and molecular determinants. *Biol Cell* 2004; **96**: 3–17.
28. Crompton M, Virji S, Ward JM. Cyclophilin-d binds strongly to complexes of the voltage-dependent anion channel and the adenine nucleotide translocase to form the permeability transition pore. *Eur J Biochem* 1998; **258**: 729–735.
29. Garcia-Dorado D, Ruiz-Meana M, Inserte J, Rodriguez-Sinovas A, Piper HM. Calcium-mediated cell death during myocardial reperfusion. *Cardiovasc Res* 2012; **94**: 168–180.
30. Mendes CC, Gomes DA, Thompson M, Souto NC, Goes TS, Goes AM *et al.* The type III inositol 1,4,5-trisphosphate receptor preferentially transmits apoptotic Ca^{2+} signals into mitochondria. *J Biol Chem* 2005; **280**: 40892–40900.
31. Anger M, Lompre AM, Vallot O, Marotte F, Rappaport L, Samuel JL. Cellular distribution of Ca^{2+} pumps and Ca^{2+} release channels in rat cardiac hypertrophy induced by aortic stenosis. *Circulation* 1998; **98**: 2477–2486.
32. Frolkis VV, Frolkis RA, Mkhitarian LS, Fraifeld VE. Age-dependent effects of ischemia and reperfusion on cardiac function and Ca^{2+} transport in myocardium. *Gerontology* 1991; **37**: 233–239.
33. Gysembergh A, Lemaire S, Piot C, Sportouch C, Richard S, Kloner RA *et al.* Pharmacological manipulation of Ins(1,4,5)p3 signaling mimics preconditioning in rabbit heart. *Am J Physiol* 1999; **277**: H2458–H2469.
34. Wieckowski MR. The role of mitochondrial permeability transition pore in physiology and pathology of the cell]. *Postepy Biochem* 2008; **54**: 71–81.
35. Obame FN, Plin-Mercier C, Assaly R, Zini R, Dubois-Rande JL, Berdeaux A *et al.* Cardioprotective effect of morphine and a blocker of glycogen synthase kinase 3 beta, sb216763 [3-(2,4-dichlorophenyl)-4(1-methyl-1 *h*-indol-3-yl)-1 *h*-pyrrole-2,5-dione], via inhibition of the mitochondrial permeability transition pore. *J Pharmacol Exp Ther* 2008; **326**: 252–258.
36. Li J, Gao E, Vite A, Yi R, Gomez L *et al.* Alpha-catenins control cardiomyocyte proliferation by regulating yap activity. *Circ Res* 2014; **116**: 70–79.
37. Palmer AE, Jin C, Reed JC, Tsien RY. Bcl-2-mediated alterations in endoplasmic reticulum Ca^{2+} analyzed with an improved genetically encoded fluorescent sensor. *Proc Natl Acad Sci USA* 2004; **101**: 17404–17409.
38. Gomez L, Chavanis N, Argaud L, Chalabreysse L, Gateau-Roesch O, Ninet J *et al.* Fas-independent mitochondrial damage triggers cardiomyocyte death after ischemia–reperfusion. *Am J Physiol Heart Circ Physiol* 2005; **289**: H2153–H2158.
39. Gomez L, Paillard M, Price M, Chen Q, Teixeira G, Spiegel S *et al.* A novel role for mitochondrial sphingosine-1-phosphate produced by sphingosine kinase-2 in PTP-mediated cell survival during cardioprotection. *Basic Res Cardiol* 2011; **106**: 1341–1353.
40. Gomez L, Thibault H, Gharib A, Dumont JM, Vuagniaux G, Scalfaro P *et al.* Inhibition of mitochondrial permeability transition improves functional recovery and reduces mortality following acute myocardial infarction in mice. *Am J Physiol Heart Circ Physiol* 2007; **293**: H1654–H1661.

Supplementary Information accompanies this paper on Cell Death and Differentiation website (http://www.nature.com/cdd)